Systems/Circuits

Laminar Origin of Corticostriatal Projections to the Motor Putamen in the Macaque Brain

Elena Borra, Marianna Rizzo, Marzio Gerbella, Stefano Rozzi, and Giuseppe Luppino
Università di Parma, Dipartimento di Medicina e Chirurgia, Parma, 43125, Italy

In the macaque brain, projections from distant, interconnected cortical areas converge in specific zones of the striatum. For example, specific zones of the motor putamen are targets of projections from frontal motor, inferior parietal, and ventrolateral prefrontal hand-related areas and thus are integral part of the so-called "lateral grasping network." In the present study, we analyzed the laminar distribution of corticostriatal neurons projecting to different parts of the motor putamen. Retrograde neural tracers were injected in different parts of the putamen in 3 *Macaca mulatta* (one male) and the laminar distribution of the labeled corticostriatal neurons was analyzed quantitatively. In frontal motor areas and frontal operculum, where most labeled cells were located, almost everywhere the proportion of corticostriatal labeled neurons in layers III and/or VI was comparable or even stronger than in layer V. Furthermore, within these regions, the laminar distribution pattern of corticostriatal labeled neurons largely varied independently from their density and from the projecting area/sector, but likely according to the target striatal zone. Accordingly, the present data show that cortical areas may project in different ways to different striatal zones, which can be targets of specific combinations of signals originating from the various cortical layers of the areas of a given network. These observations extend current models of corticostriatal interactions, suggesting more complex modes of information processing in the basal ganglia for different motor and nonmotor functions and opening new questions on the architecture of the corticostriatal circuitry.

Key words: **basal ganglia; layer VI; motor control; primates; striatal input channels; striatum**

Significance Statement

Projections from the ipsilateral cerebral cortex are the major source of input to the striatum. Previous studies have provided evidence for distinct zones of the putamen specified by converging projections from specific sets of interconnected cortical areas. The present study shows that the distribution of corticostriatal neurons in the various layers of the primary motor and premotor areas varies depending on the target striatal zone. Accordingly, different striatal zones collect specific combinations of signals from the various cortical layers of their input areas, possibly differing in terms of coding, timing, and direction of information flow (e.g., feed-forward, or feed-back).

Introduction

Projections from the ipsilateral cerebral cortex are the major source of input to the striatum, the main input station of the basal ganglia (cortico-basal ganglia-thalamo-cortical) loop.

According to early models, different striatal territories are a target of specific cortical regions and in turn are at the origin of largely segregated basal ganglia-thalamo-cortical loops (Alexander et al., 1986). Subsequent studies confirmed this view but also showed up a finer modular organization in which each main loop consists of several largely segregated closed subloops. In this view, each subloop originates from, and projects to, individual cortical areas or limited sets of functionally related areas and involves distinct, relatively restricted striatal zones, which have been referred to as "input channels" (Strick et al., 1995; Middleton and Strick, 2000). The various subloops, because of their differential cortical origin and termination, could be functionally distinct and their definition is thus essential for understanding the mode of information processing in the basal ganglia for different motor and nonmotor functions.

In this context, one important aspect is the definition of the way in which cortical areas or sectors contribute to the projections to a specific striatal zone in terms of laminar origin of their projections. Based on studies conducted in different animal species, it is largely agreed that corticostriatal (CSt) neurons are typically located mostly in layer V and, in some cases, layer III of most cortical areas (see Gerfen and Bolam, 2010). In the

Received June 9, 2020; revised Dec. 1, 2020; accepted Dec. 4, 2020.

Author contributions: E.B., M.G., S.R., and G.L. designed research; E.B., M.R., M.G., S.R., and G.L. performed research; E.B., M.R., and G.L. analyzed data; E.B. and G.L. wrote the paper; M.G. and S.R. edited the paper.

This work was supported by: Programme "FIL-Quota Incentivante" of University of Parma and co-sponsored by Fondazione Cariparma; Ministero dell'Istruzione, dell'Università e della Ricerca (Grant number: PRIN 2017, n°2017KZNZLN_002). The 3D reconstruction software was developed by CRS4, Pula, Cagliari, Italy.

The authors declare no competing financial interests.

Correspondence should be addressed to Elena Borra at elena.borra@unipr.it.

https://doi.org/10.1523/JNEUROSCI.1475-20.2020

macaque brain, based on retrograde tracer injections in the caudate, the contribution of layer III in the temporal cortex and PFC was found to be correlated with the density of CSt-labeled cells (Arikuni and Kubota, 1986; Saint-Cyr et al., 1990). Recently, this view has been seriously challenged by data of Griggs et al. (2017), based on retrograde tracer injections in the head or the tail of the macaque caudate showing that: (1) in the temporal cortex, laminar patterns of CSt projections from a given cortical sector markedly differ according to the striatal target; and (2) layer VI can heavily contribute to the projections to specific striatal targets.

Accordingly, laminar patterns of CSt projections could be more complex than previously considered and could represent an important variable to evaluate in defining the possible contribution of cortical areas to the projections to a specific putaminal zone.

In the present study, we addressed this issue focusing on the macaque CSt projections to the so-called "motor putamen," that is, that part of the putamen that is a target of massive projections from the various subdivisions of the primary motor and premotor areas (frontal motor areas). Previous studies have provided evidence for converging projections from different sets of frontal and cingulate motor areas in different parts of the motor putamen (Takada et al., 1998; Nambu, 2011). Recent data (Gerbella et al., 2016), showing that projections from hand-related ventral premotor, inferior parietal, and ventrolateral prefrontal areas forming the "lateral grasping network" (Borra et al., 2017) overlap in two distinct putaminal zones, suggested an even more complex pattern of converging input for parallel processing of different aspects of motor and nonmotor functions.

Specifically, based on retrograde tracer injections in different parts of the motor putamen, we have analyzed the laminar distribution of the labeled CSt neurons. Main aims were as follows: (1) to quantify the contribution of the different cortical layers to the projections to a given relatively restricted putaminal zone; (2) to see whether these contributions vary within the various labeled cortical regions; and (3) to assess whether possible differences in laminar distribution patterns are related to the labeled cells density, the cortical area, or the target putaminal zone.

Materials and Methods

Subjects, surgical procedures, and selection of the injection sites

The experiments were conducted in three *Macaca mulatta* (Cases 61, 71, and 75, one male), in which retrograde neural tracers were injected in the putamen. Animal handling as well as surgical and experimental procedures complied with the European law on the humane care and use of laboratory animals (directives 86/609/EEC, 2003/65/CE, and 2010/63/EU) and Italian laws in force regarding the care and use of laboratory animals (D.L. 116/92 and 26/2014), and were periodically approved by the Veterinarian Animal Care and Use Committee of the University of Parma and authorized by the Italian Ministry of Health.

Before the injection of neural tracers, we obtained scans of each brain using MRI (Cases 71 and 75: 7 T General Electric; Case 61: 0.22 T Paramed Medical Systems) to calculate the stereotaxic coordinates of the putaminal target regions and the best trajectory of the needle to reach it.

Under general anesthesia (Cases 61 and 71: Zoletil, initial dose 20 mg/kg, i.m., supplemental 5-7 mg/kg/h, i.m., or ketamine, 5 mg/kg i.m. and medetomidine, 0.08-0.1 mg/kg i.m.; Case 75: induction with ketamine 10 mg/kg, i.m. followed by intubation, isoflurane 1.5%-2%) and aseptic conditions, each animal was placed in a stereotaxic apparatus and an incision was made in the scalp. The skull was trephined to remove the bone, and the dura was opened to expose a small cortical region. After tracer injections, the dural flap was sutured, the bone was replaced, and the superficial tissues were sutured in layers. During surgery, hydration was maintained with saline, and heart rate, blood pressure, respiratory depth, and body temperature were continuously monitored. Upon recovery from anesthesia, the animals were returned to their home cages and closely observed. Dexamethasone (0.5 mg/kg, i.m.) and prophylactic broad-spectrum antibiotics (e.g., ceftriaxone 80 mg/kg, i.m.) were administered preoperatively and postoperatively, as were analgesics (e.g., ketoprofen 5 mg/kg i.m.).

Table 1. Animals used, location of injection sites in the putamen, and type and amount of injected tracers

Case	Species	Sex	Age (years)	Weight (kg)	Hemisphere	AP[a]	Tracer	Amount (μl)
61	*M. mulatta*	F	6	4.5	R	1	CTBg 1%	2
71	*M. mulatta*	F	6.5	3.3	L	−2	FB 3%	0.3
					R	2	CTBg 1%	1
75	*M. mulatta*	M	6	3.5	R	0	CTBg 1%	1

[a]AP level according to the digital atlas of Reveley et al. (2017) in which AP = 0 is at the level of the AC.

Tracer injections and histologic procedures

Based on stereotaxic coordinates, the neural tracers Fast Blue (FB, 3% in distilled water, Dr. Illing Plastics) and cholera toxin B subunit, conjugated with Alexa488 (CTB green [CTBg]; 1% in 0.01 M PBS at pH 7.4, Invitrogen, Thermo Fisher Scientific) were slowly pressure-injected through a stainless-steel 31 gauge beveled needle attached through a polyethylene tube to a Hamilton syringe. In Cases 71 and 75, the injection needle was lowered to the putamen within a guiding tube, to avoid tracer spillover in the white matter. Table 1 summarizes the locations of the injections, the injected tracers, and the amounts injected.

After appropriate survival periods following the injections (28 d for FB and 14 d for CTBg), each animal was deeply anesthetized with an overdose of sodium thiopental and perfused through the left cardiac ventricle consecutively with saline (~2 L in 10 min), 3.5% formaldehyde (5 L in 30 min), and 5% glycerol (3 L in 20 min), all prepared in 0.1 M PB, pH 7.4. Each brain was then blocked coronally on a stereotaxic apparatus, removed from the skull, photographed, and placed in 10% buffered glycerol for 3 d and 20% buffered glycerol for 4 d. In Case 75, the right inferotemporal cortex was removed for other experimental purposes. Finally, each brain was cut frozen into coronal sections of 60 μm (Cases 61 and 75) or 50 μm (Case 71) thickness.

In all cases, sections spaced 300 μm apart (i.e., one section in each repeating series of 5 in Cases 61 and 75 and one in series of 6 in Case 71) were mounted, air-dried, and quickly coverslipped for fluorescence microscopy. Another series of each fifth section (sixth in Case 71) was processed for visualizing CTBg with immunohistochemistry. Specifically, endogenous peroxidase activity was eliminated by incubation in a solution of 0.6% hydrogen peroxide and 80% methanol for 15 min at room temperature. The sections were then incubated for 72 h at 4°C in a primary antibody solution of rabbit anti-Alexa-488 (1:15,000, Thermo Fisher Scientific; RRID:AB_221544) in 0.5% Triton, 5% normal goat serum in PBS, and for 1 h in biotinylated secondary antibody (1:200, Vector Laboratories) in 0.3% Triton, 5% normal goat serum in PBS. Finally, CTBg labeling was visualized using the Vectastain ABC kit and then a solution of DAB (50 mg/100 ml; Sigma Millipore), 0.01% hydrogen peroxide, 0.02% cobalt chloride, and 0.03% nickel ammonium sulfate in 0.1 M PB. In Case 75, a subset of sections spaced 1200 μm immunostained for CTBg were then incubated overnight at room temperature in a primary antibody solution of rabbit anti-NeuN (1:5000, Cell Signaling Technology; RRID:AB_2630395) in 0.3% Triton, 5% normal goat serum in PBS, and for 1 h in biotinylated secondary antibody (1:100, Vector Laboratories) in 0.3% Triton, 5% normal goat serum in PBS. Finally, NeuN-positive cells were visualized using the Vectastain ABC kit and DAB as a chromogen. With this protocol, in the same tissue sections, CTBg labeling was stained black and NeuN-positive cells were stained brown. In Case 75, an additional subset of sections spaced 1200 μm through the frontal lobe were incubated in a primary antibody solution of anti-Alexa-488 and in a biotinylated secondary antibody solution as described above, followed by incubation for 1 h in a solution of streptavidin Alexa-488-conjugated (1:500, Invitrogen) in PBS with 0.5% Triton. The same sections were then incubated overnight at room temperature in a primary antibody solution of mouse monoclonal SMI-32

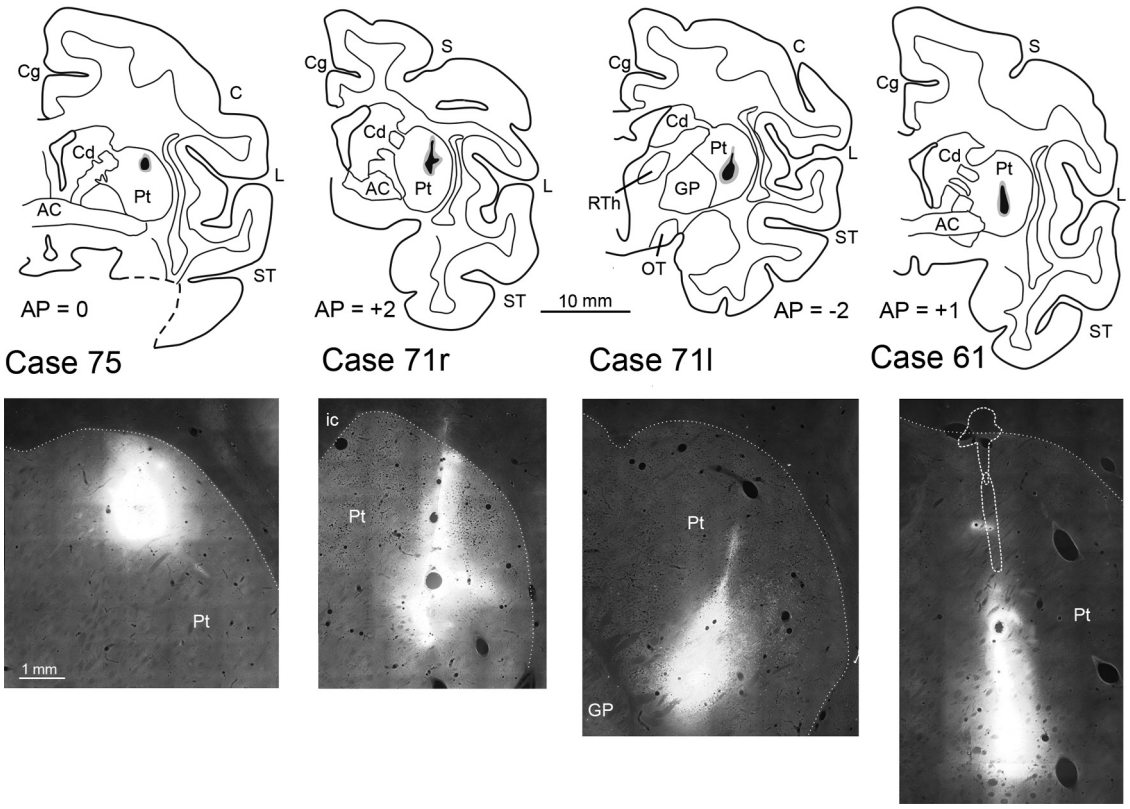

Figure 1. Location of the injection sites. Top, Drawings of coronal sections showing the location of the injection sites in the putamen depicted as a black zone corresponding to the core, surrounded by a gray zone corresponding to the halo. All sections are shown as from a right hemisphere. The AP level of the sections is indicated in relation to the digital atlas of Reveley et al. (2017), in which AP = 0 is at the level of the AC. Bottom, Fluorescence photomicrographs of the injection sites in the putamen. Scale bar in Case 75 applies to all. Dashed lines in the injection site of Case 61 indicate the deposit of the tracer in adjacent sections. C, Central sulcus; Cd, caudate nucleus; Cg, cingulate sulcus; GP, globus pallidus; ic, internal capsule; L, lateral fissure; OT, optic tract; Pt, putamen; RTh, reticularis thalami; S, spur of the arcuate sulcus; ST, superior temporal sulcus.

(1:5000; Covance; RRID:AB_2315331), in PBS with 0.5% Triton and 2% normal goat serum, and for 1 h in a secondary antibody solution of goat anti-mouse conjugated with Alexa-568 (1:500, Invitrogen, Thermo Fisher Scientific), in PBS with 0.3% Triton and 2% normal goat serum. In all cases, one series of each fifth section (sixth section in Case 71) was stained with the Nissl method (0.1% thionine in 0.1 M acetate buffer, pH 3.7).

Data analysis

Injection sites, distribution of retrogradely labeled neurons, and areal attribution of the labeling. The criteria used for defining the injection site core and halo and identifying FB and CTBg labeling have been described previously (Luppino et al., 2003; Rozzi et al., 2006). The injection sites of Cases 71 and 75 were completely restricted to the putamen. In Case 61, the CTBg injection site had some involvement (<500 μm) of the white matter just above the putamen (Fig. 1). This white matter involvement, given its minimal extent and location in close contact with the putamen and considering that CTB is characterized by a limited uptake by axons of passage (Lanciego, 2015), should not have affected the results from this case, which were fully comparable with those of the other cases.

The distribution of retrograde labeling in the cortex was analyzed in sections every 300 μm and plotted in sections every 1200 μm (Cases 61, 71r, and 75) or 600 μm (Cases 71l) together with the outer and inner cortical borders, using a computer-based charting system. Data from individual sections were also imported into the 3D reconstruction software (Demelio et al., 2001) providing volumetric reconstructions of the monkey brain, including connectional and architectonic data.

The criteria and maps adopted for the areal attribution of the labeling were similar to those adopted in previous studies (see Borra et al., 2017). Specifically, the attribution of the labeling to the frontal motor, cingulate, and opercular frontal areas was made according to architectonic criteria previously described (Matelli et al., 1985, 1991; Belmalih et al., 2009).

Quantitative analysis and laminar distribution of the labeling. In all cases, the number of labeled neurons plotted in the ipsilateral hemisphere was counted and the cortical input to the injected putaminal zone was then expressed in terms of the percentage of labeled neurons found in a given cortical subdivision, with respect to the overall cortical labeling found for each tracer injection.

In all cases, the laminar distribution of the labeled cells was analyzed quantitatively in pairs or triplets of close sections (spaced 300-600 μm), taken at different rostrocaudal levels through the frontal motor and cingulate cortex and the frontal opercular cortex (Fig. 2). Given that, in Cases 75 and 71r, the labeling distribution was quite similar, the same levels (two sections/level) were selected: the first level (A) was taken through F1, the second (B) through the caudal part of F3, the third (C) through the middle part of F3, and the fourth (D) through the rostralmost part of F3. In Case 61, the labeling involved more rostral cortical territories than in Cases 75 and 71r; thus, the caudalmost level analyzed was level B, and it was possible to analyze a further rostral level (E) through areas F6 and F7. In Case 71l, the labeling was dense in relatively restricted cortical sectors; thus, the analysis was focused on these regions, at levels corresponding to B, C, and D, and was conducted in two (level D) or three (levels B and C) sections spaced 600 μm.

Quantitative analysis was also conducted in parietal, insular, and prefrontal sectors selected based on the distribution of the labeling in each case. For analyzing these regions, given that the laminar distribution of the labeling was apparently very constant, cortical sectors of 2 mm from two close sections (spaced 300-600 μm) were analyzed.

The selected sections were photographed at 100× magnification through a digital camera incorporated into the microscope with an automatic acquisition system (NIS-Element; Nikon), and labeled neurons were plotted on the microphotographs. In the frontal sections of Cases

61, 71r, and 75, the entire extent of the frontal motor and cingulate cortex and the opercular frontal cortex was subdivided in 500-μm-wide cortical traverses perpendicular to the cortical surface and running through the entire cortical thickness, from the pial surface to the gray-white matter border. The width of the traverses was defined along a line running at the level of the layers III-V border. In the frontal sections of Case 71l and in the sections through the parietal, insular, and PFC in all cases, where the labeling was in general less rich, cortical traverses 1-mm-wide were defined in limited cortical sectors. Furthermore, microphotographs of immediately adjacent Nissl-stained sections were overlaid, and borders between different cortical layers were then transferred on the plots. Two types of analyses were conducted on the distribution of the labeled neurons. The first analysis aimed to obtain an estimate of the variations in overall richness of the labeling within and across the various labeled cortical sectors. To this purpose, we have first considered the total number of labeled cells observed in each traverse, in the entire cortical thickness. Then, to compensate for differences in the number of labeled cells because of variations of the cortical thickness between different areas or to oblique cutting of the cortical mantle, the total number of labeled cells was divided by the cortical thickness, measured from the pial surface to the gray-white matter border, expressed in millimeters. Thus, the richness of the labeling ("density") was expressed for each traverse in terms of number of labeled cells/mm cortical thickness. The second analysis aimed to quantify the proportion of CSt-labeled cells observed in the various layers. To this aim, for each traverse, the labeling was expressed in terms of percentage of labeled neurons localized in layers II-III, V, and VI.

The distribution of labeled neurons was also analyzed qualitatively across consecutive sections to exclude the possibility that the observed laminar distribution patterns of the labeling were only apparent because of an oblique cutting of the cortical mantle.

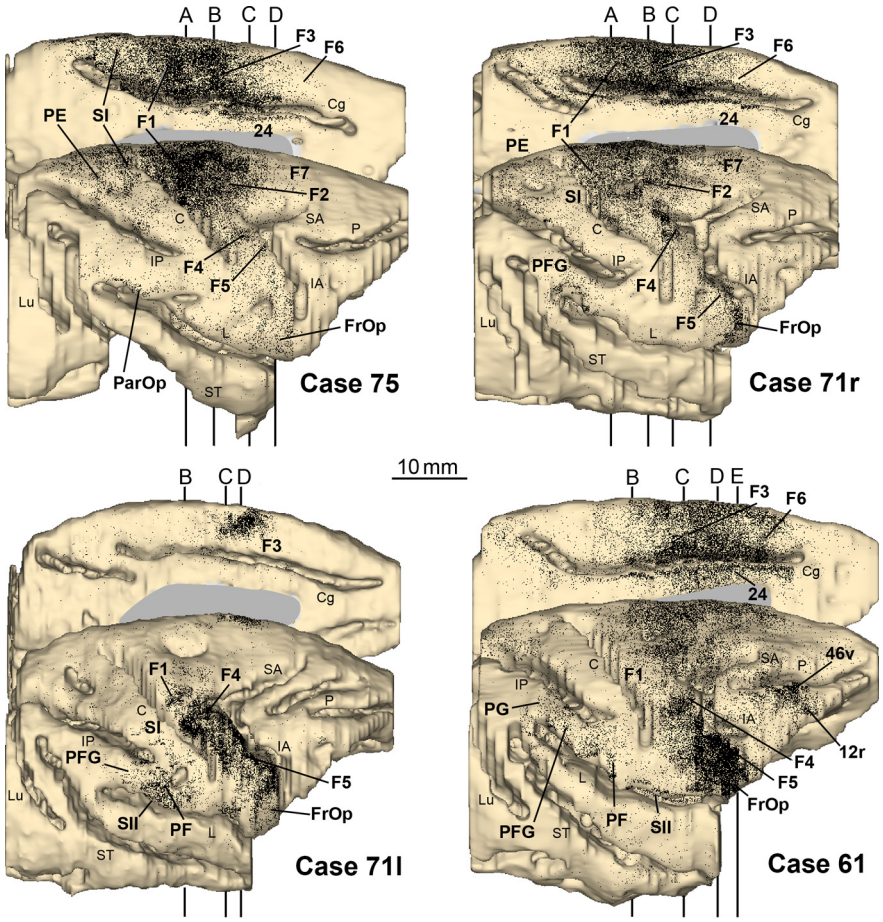

Figure 2. Distribution of the cortical labeling observed after injections in the putamen. The distribution of the retrograde labeling is shown in dorsolateral and medial views of the 3D reconstructions of the injected hemispheres in which each dot corresponds to one labeled neuron. In each reconstruction, solid lines indicate the levels (A-E) of the sections selected for the quantitative analysis. For the sake of comparison, also Case 71l is shown as right. FrOp, Frontal operculum; IA, inferior arcuate sulcus; IP, intraparietal sulcus; Lu, lunate sulcus; P, principal sulcus; ParOp, parietal operculum; SA, superior arcuate sulcus. Other abbreviations as in Figure 1.

Results

Location of the injection sites and general distribution of labeled CSt neurons in the ipsilateral hemisphere

All injections used for this study involved the putaminal region overlying the crossing of the anterior commissure (AC) at different dorso-ventral (DV) levels (Table 1; Fig. 1). In Cases 75 and 71r, the injection sites were located in a dorsal and a mid-dorsal part of the putamen, respectively, at about the antero-posterior (AP) level of the AC (Case 75), or slightly rostral (Case 71r). According to the putaminal motor somatotopy (e.g., Alexander and DeLong, 1985; Nambu, 2011), the injection site in Case 75 could correspond mostly to the trunk-leg motor representation and in Case 71r to the arm and trunk-leg motor representation. In Cases 71l and 61, the injection sites were located more ventrally in the putamen, 2 mm caudal and 1 mm rostral to the center of the AC, respectively. In Case 71l, the injection site could overlap with the hand and mouth motor representation. In Case 61, it extended for ~4 mm in DV direction and the ventral part could at least partially overlap with the rostral "hand-related input channel" (Gerbella et al., 2016).

Table 2. Regional distribution (%) and total number (*n*) of labeled neurons observed following tracer injections in the motor putamen

Case	Prefrontal	Cingulate	Frontal motor	Parietal	Insula	Temporal	No. of cells
75	0.7	19.4	61.7	16.7	1.6	—	59,653
71r	1.6	21.9	61.6	11.9	3	—	60,757
71l	0.5	3.4	75.5	18.6	1.2	0.8	36,628
61	8.4	18.3	57	7.5	6.1	2.7	105,724

As expected, in all cases, the majority of labeled cells was located in frontal motor areas (57%-75% of the labeled cells; Table 2) with additional, in several cases relatively robust, projections from other cortical regions, and their distribution in the ipsilateral hemisphere largely varied depending on the location of the injection site (Figs. 2 and 3).

In Cases 75 and 71r, the regional distribution of the labeling was quite similar: in both cases, ~62% of the labeled cells were located within frontal motor areas, ~19%-22% in the cingulate cortex, and ~12%-17% in the parietal cortex. In both cases, the strongest input originated from F1 (primary motor cortex), mostly from the dorsal and medial part, and a very rich labeling

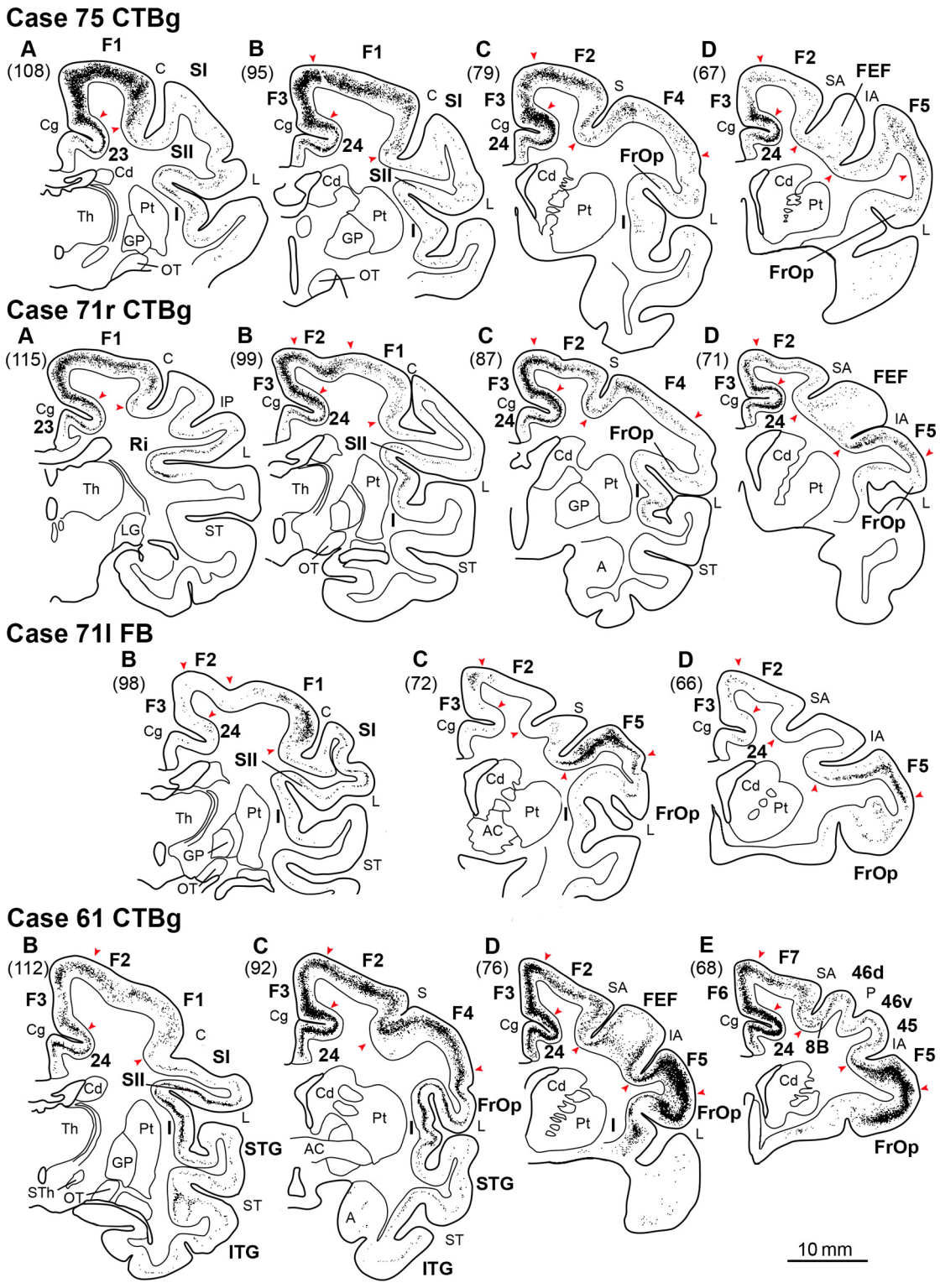

Figure 3. Distribution of the cortical labeling in one representative section from each level selected for the quantitative analysis. Section drawings are in a caudal to rostral order (A-E) and were taken at the levels shown in Figure 2. Section number is indicated in brackets. Arrowheads indicate borders of frontal motor areas. Subcortical labeling is not shown. A, Amygdala; FEF, frontal eye field; I, insula; ITG, inferior temporal gyrus; LG, lateral geniculate nucleus; Ri, retro-insular cortex; STG, superior temporal gyrus; STh, subthalamic nucleus; Th, thalamus. Other abbreviations as in Figures 1 and 2.

involved the entire extent of F3 (supplementary motor area) and area 24c/d (cingulate motor areas) mostly in the caudal part, corresponding to area 24d (Table 3). Relatively strong projections originated also from F2 and, in Case 71r, in which the injection site extended more ventrally, also from F5. In the parietal cortex, in both cases, most of the labeling was in the dorsal part of the primary somatosensory area (SI) and of area PE and, in Case 71r, also in area PFG.

In Case 71l, the labeling was much weaker in the cingulate cortex and mostly confined to the frontal motor (76%) and

Table 3. Distribution (%) in the frontal and cingulate motor cortex and in the frontal operculum of labeled neurons observed following tracer injections in the motor putamen

Case	24c/d	F6	F7	F3	F2	Frontal operculum	F5	F4	F1
75	14.4	0.8	0.3	12.7	7.1	2.2	2.5	2.0	34.1
71r	14.4	0.8	0.5	13.2	6.5	2.4	7.9	3.3	26.9
71l	2.5	0.1	—	6.9	0.7	7.6	33.4	8.2	18.6
61	12.3	3.7	1.2	10.6	9.3	16.5	10	3.0	2.7

parietal (19%) cortex (Table 2). In the frontal cortex, the labeling was very strong in the ventral premotor cortex, mostly in F5, also extending in the frontal operculum, and in the mid-ventral part of F1 (Table 3), as expected from the location of the injection site. Relatively robust labeling was observed in the rostral part of F3, likely involving the arm and face representation (Luppino et al., 1991). In the parietal cortex, labeled cells were mostly distributed in the ventral part of SI, and in secondary somatosensory area (SII), PF, PFG, and the anterior intraparietal area (AIP).

In Case 61, the cortical labeling was more extensive than in the other 3 cases, likely because of its more rostral location and relatively large DV extent. Specifically, the labeling very densely involved the ventral premotor, the ventrolateral PFC, and the IPL areas PFG, PG, and AIP, which likely reflects involvement of the rostral "hand-related input channel." The labeling densely involved also F3 (mostly the mid-rostral part), F2, and 24c/d and, less densely, areas F6, 24a/b and the insula (Tables 2 and 3).

Laminar distribution of CSt-labeled cells in the frontal motor, cingulate, and frontal opercular cortex

As shown in detail below, in general, the laminar distribution pattern of the labeled CSt cells in the frontal motor and opercular cortex markedly differed across the various labeled zones and very rarely showed the pattern commonly described in the primate brain, characterized by CSt cells almost completely confined to layer V. For example, in the frontal motor cortex, in only 8% of the 1009 cortical bins (500-μm-wide) analyzed in 36 sections from all cases, labeled cells in layer V were >66% and in 58% of the bins they were <50%. Indeed, labeled cells almost everywhere in these regions tended to distribute over almost the entire cortical depth, involving, at a variable extent, layers III, V, and VI. Noteworthy, there were also labeled CSt neurons in the underlying white matter, which have been described in a previous study (Borra et al., 2020).

Figure 4 shows the results of the quantitative analysis conducted in sections through F1, which was very richly labeled in Cases 75, 71r, and 71l. In sections sampled from Cases 75 and 71r, taken caudally in F1 (Figs. 2 and 3, level A), in the granular cingulate area 23 the labeling by far predominantly involved layer V, as in most of the sampled bins labeled cells in this layer were >80% in Case 75 and >90% in Case 71r (Fig. 5*A*, *B*). In Case 75, at the transition of area 23 with F1, the laminar distribution pattern radically changed, as the proportion of labeled cells in layers III and VI increased considerably (Fig. 5*C*). For example, in section 108, there were ~12-13 mm (bins 16-41) in which the proportion of layer V labeled cells was ~40% and that of either layer III or layer VI was ~30%, whereas in section 109, the proportion of layer VI labeled cells tended to be ~20%. Interestingly, this pattern remained unchanged despite clear changes in labeling density, even when it abruptly halved in the range of very few bins (e.g., bins 28-31 in section 108). In Case 71r, the laminar distribution pattern in a sector of F1, similar to that sampled in Case 75, was somewhat different: the proportion of labeled cells in layer V tended to be higher than that in layers III and VI, though remaining for the whole extent of F1 in both the sampled sections at ~50%. In Case 71l, F1 was sampled in a triplet of close sections in a more lateral part (Figs. 2 and 3, level B), mostly in the bank of the central sulcus, where the labeling in this area was richest. In all three samples, the proportion of labeled cells in layer VI tended to be quite low, but that in layer III was as high or, in several bins, even higher than in layer V, being >50% in 8 mm of 13 mm sampled (Fig. 5*E*). A similar pattern was also observed in bins located in the bank of the central sulcus in Case 75.

In all cases, layer V labeled cells in F1 were all relatively small and tended to be densely packed mainly in the upper part of the layer, corresponding to sublayer Va. In Case 75, SMI-32 immunofluorescence, which reveals neurofilament proteins expressed in subpopulations of layer III and V pyramids (Hof and Morrison, 1995), including the larger ones in layer Vb in the frontal motor cortex (Geyer et al., 2000; Belmalih et al., 2009), showed that CTBg labeled neurons, though invading layer Vb, were considerably smaller than larger SMI-32-immunopositive pyramids (compare Fig. 5*C*,*D*). The analysis of these double-labeled sections also clearly showed that a high proportion of CTBg-labeled cells was located well below the large layer Vb pyramids, in layer VI.

Rostral to F1, the cingulate area 24c/d and the medial premotor cortex corresponding to F3 were sampled at different AP levels together with the adjacent sectors of F1 or F2 (levels B, C, and D; Figs. 6-8). Figure 7 shows the results of the analysis conducted in pairs of sections taken in all cases at about the middle of F3, possibly corresponding to the arm representation of this area (level C). In area 24c/d, labeled cells were mainly located in layer V, although, especially in Case 61, in several bins, the proportion of cells located in layers III and VI was ~40%. In Cases 75 and 71r, the laminar distribution pattern of labeled cells in F3 (Fig. 5*F*) was substantially similar to that observed in F1. In Case 61, the percentage of layer V-labeled cells was in most of the bins ~40%, in layer III tended to match that of layer V, whereas in layer VI it was lower and quite variable. In Case 71l, relatively dense labeling was observed in a restricted zone in the mid-rostral part of F3. Here, in two of three sampled sections, labeled cells tended to be located mainly in layer V (~60%), whereas in one section the proportion of labeled cells in layer VI matched that in layer V. In F2, the density of labeled cells tended to be lower than in F3 and their laminar distribution tended to be similar to that observed in F3, though more variable across bins. Similar laminar distribution patterns were observed in Cases 75, 71r, and 61 in the caudal part of areas 24c/d and F3 (level B; Fig. 6).

At level D (Figs. 2 and 3), through the rostralmost part of F3, at the border with F6, a different laminar distribution pattern was observed in Cases 75 and 71r, characterized by a clear increase in the percentage of labeled cells in layer V, compared with the more caudal levels (Fig. 8). In Case 61, ~40%-50% of the labeled cells were located in layer V, and the remaining were almost equally subdivided in layers III and VI.

An additional more rostral level (level E) was sampled in Case 61 through areas 24c/d and F6, where rich labeling was located (Fig. 9). The laminar distribution of the labeling was similar to that observed more caudally in area 24c/d and rostral F3.

Accordingly, as observed for F1, there were differences in the laminar origin of CSt projections from medial and dorsal premotor areas, which were not correlated with the density of the labeling, but likely with the target putaminal zone.

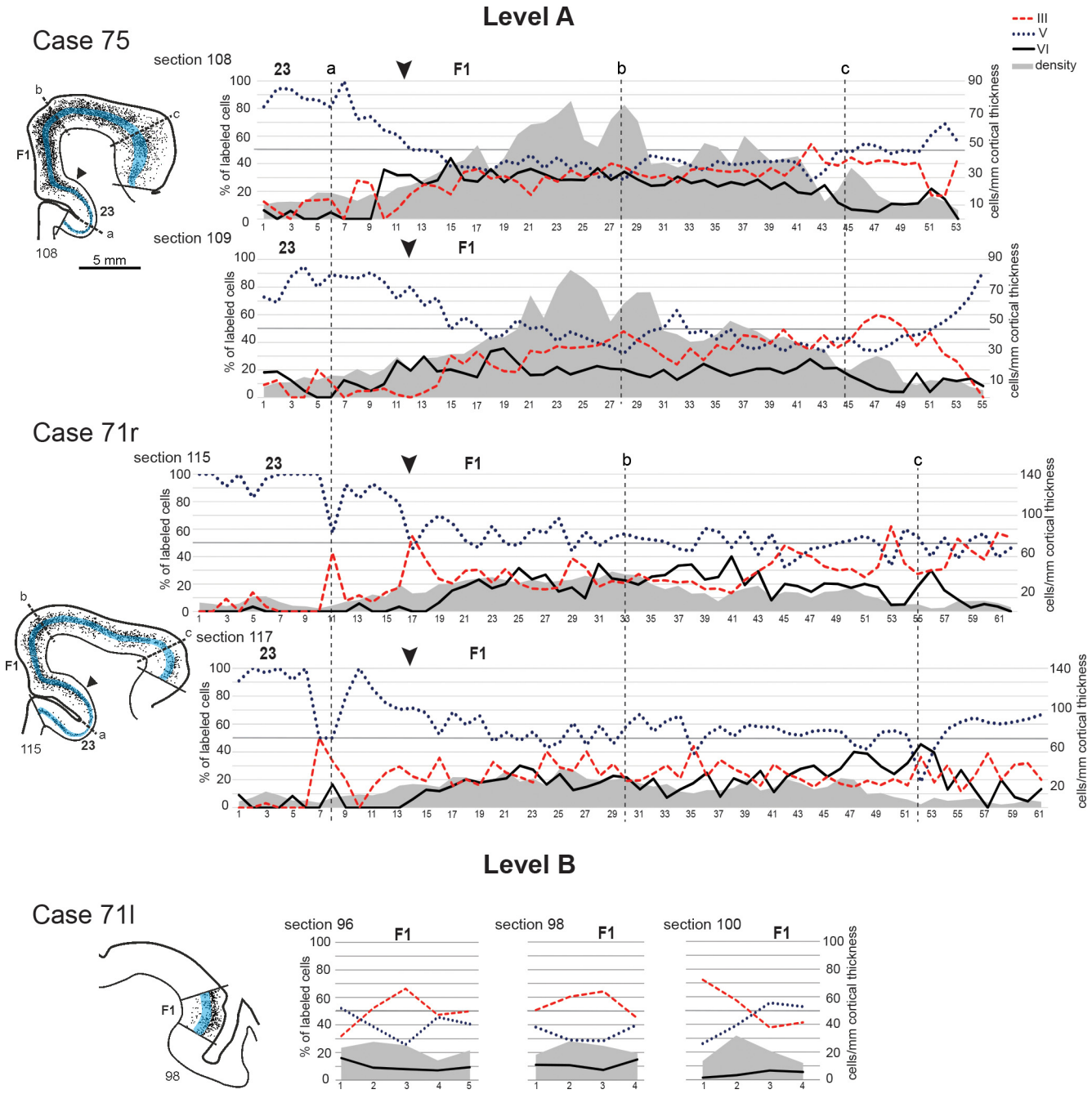

Figure 4. Percent laminar distribution and density of the retrograde labeling in F1. Graphs represent data from Cases 75, 71r (level A, 2 sections each), and 71l (level B, 3 sections). For each case, on the left, one section drawing shows the analyzed cortical sector and layer V shaded in light blue. Graphs from Cases 75 and 71r are aligned at the level of the fundus of the cingulate sulcus (a), indicated by a vertical dashed line. The other vertical dashed lines indicate the level of the medial edge of the hemisphere (b) and the shoulder of the central sulcus (c). Graphs from Case 75 and 71r represent data from 500-μm-wide bins from the region in which the labeled cell density was constantly higher than 10 labeled cells/bin/mm. In graphs from Case 71l, the bins are 1-mm-wide and located in the lateral part of F1, in the bank of the central sulcus. Arrowheads indicate the location of areal borders.

In three cases (61, 71r, and 71l), there was rich labeling also in the ventral premotor cortex (Fig. 10). In Case 61, the laminar distribution of the labeled cells in this region was examined through F5 and the frontal operculum (levels D and E) and more caudally through F4 (level C). In Cases 71l and 71r, the labeling was rich in restricted zones of F5 and F4, which were sampled at levels D and C, respectively. In Case 61, in the F5 sector buried within the postarcuate bank (subdivision F5a), labeled cells were by far predominantly located in layer V. This pattern markedly changed in the F5 sector extending on the convexity cortex (subdivision F5c), where the percentage of labeled cells located in layer VI considerably increased, matching in several bins that of layer V (~40%; Fig. 5*G*). More ventrally, in the frontal operculum, at level E, the contribution of layer VI further increased, reaching in most of the bins percent values of at least 60%, whereas more caudally (level D) tended to be similar to that observed for F5c. In F5c and in the frontal operculum, as well as in all the other frontal motor areas, labeled cells in layer VI tended to be more concentrated in the upper part of the layer and included pyramidal and nonpyramidal neurons (Fig. 5*H*). Finally, in F4 (level C), ~50% of the labeled cells was in layer V.

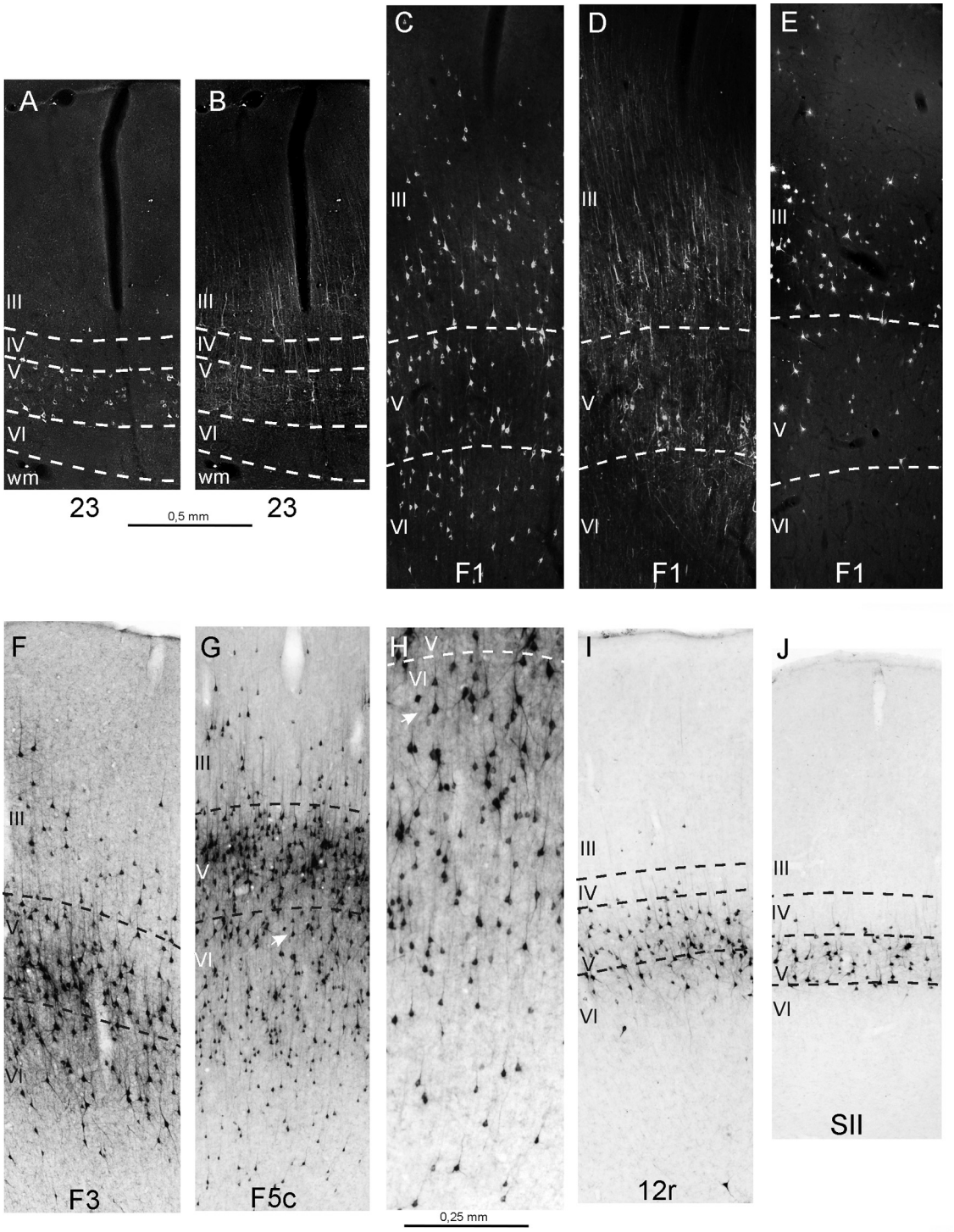

Figure 5. Examples of laminar distribution of the labeling. ***A***, ***B*** (section 110), ***C***, ***D*** (section 106), and ***F*** (section 93) are from Case 75. ***B***, ***D***, SMI-32 immunofluorescence in ***A*** and ***C***, respectively. ***E*** (section 98) is from Case 71l. ***G*** (section 76, enlarged in ***H***), ***I***, Case 61. ***J***, Case 71r.

In Cases 71l and 71r, the laminar distribution pattern observed in F5a (both cases) and in F4 (Case 71r) was very similar to that described for Case 61. In contrast, the laminar distribution pattern observed in F5c in Case 71l was markedly different from that observed in Case 61: the percentage of labeled cells in layer V was by far predominant and that of layer VI was ~10%. This observation was a further clear example that a given premotor area can project to different parts of the motor putamen with a differential contribution of the various cortical layers.

Laminar distribution of CSt-labeled cells in the parietal, insular, and PFC

Differently from what was observed in the frontal motor and cingulate cortex and in the frontal opercular cortex, in the parietal and insular cortex, the laminar distribution of the CSt-labeled cells was substantially uniform and characterized by pyramidal cells predominantly confined to layer V, with some of them in the position of layer IV. Specifically, in the parietal cortex, independently from the labeled area and from the richness of the

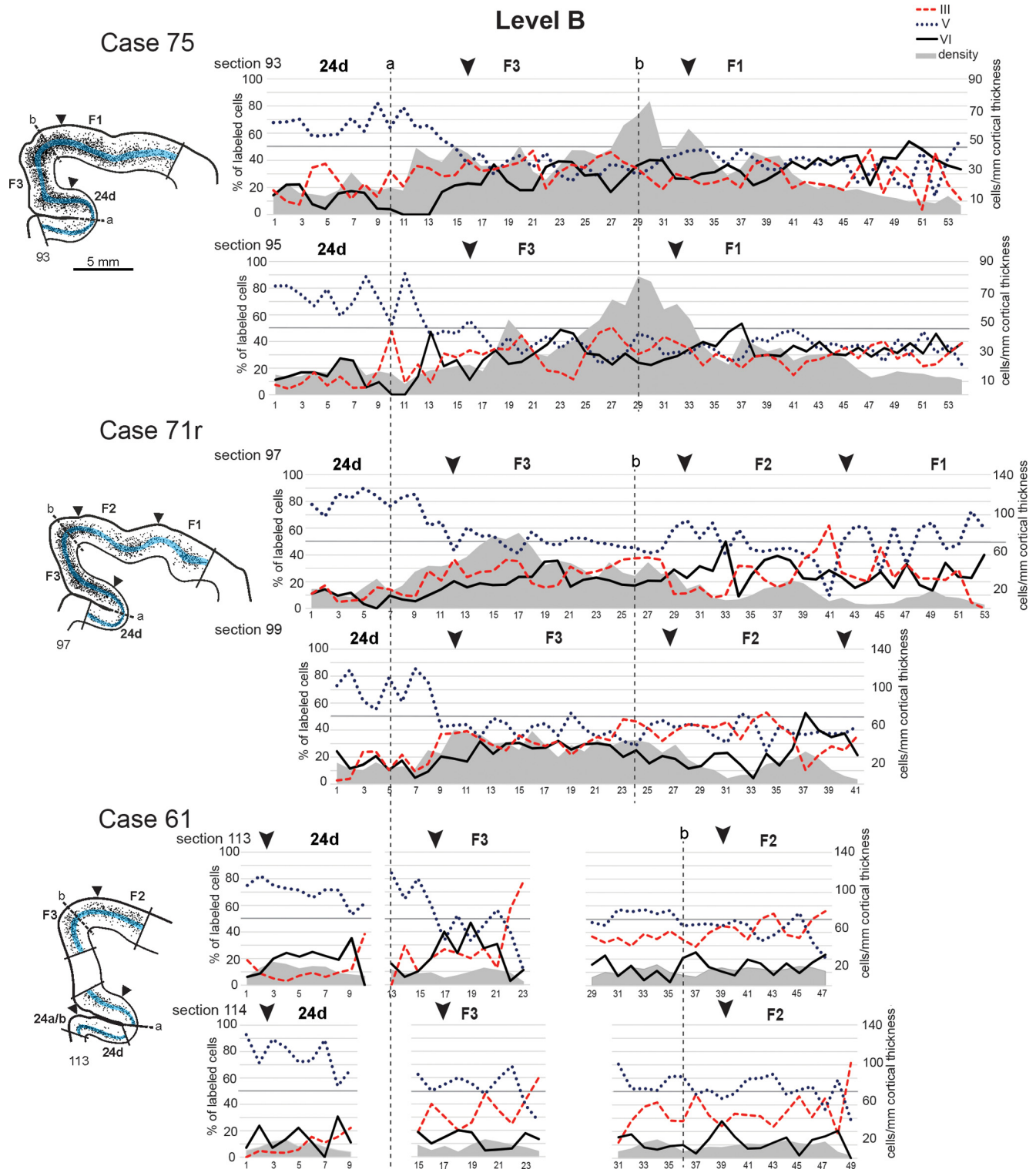

Figure 6. Percent laminar distribution and density of the retrograde labeling in the cingulate and frontal motor cortex at level B in Cases 75, 71r, and 61. Conventions as in Figure 4.

labeling, labeled cells in layer V (plus layer IV) tended to be almost everywhere >80%, with the remaining mostly localized in layer VI (Fig. 5*J*). In the insular cortex, labeled cells were by far predominantly located in layer V in Cases 75, 71r, and 71l in which the labeling was relatively poor. In Case 61, in which labeling in the insula was considerably richer, most of the labeled cells was located in layer V; and a variable, but robust, proportion was located in layer VI. This same case was the only one in which relatively rich labeling was observed in the ventrolateral PFC, more densely involving areas 46v and 12r. In this region, the majority of the labeled cells was located in layer V; but as observed in the insular cortex, there was a relatively robust contribution (up to 40% of the labeled cells) of layer VI (Fig. 5*I*).

Discussion

The present study shows that CSt projections from frontal motor areas and frontal operculum do not originate almost exclusively

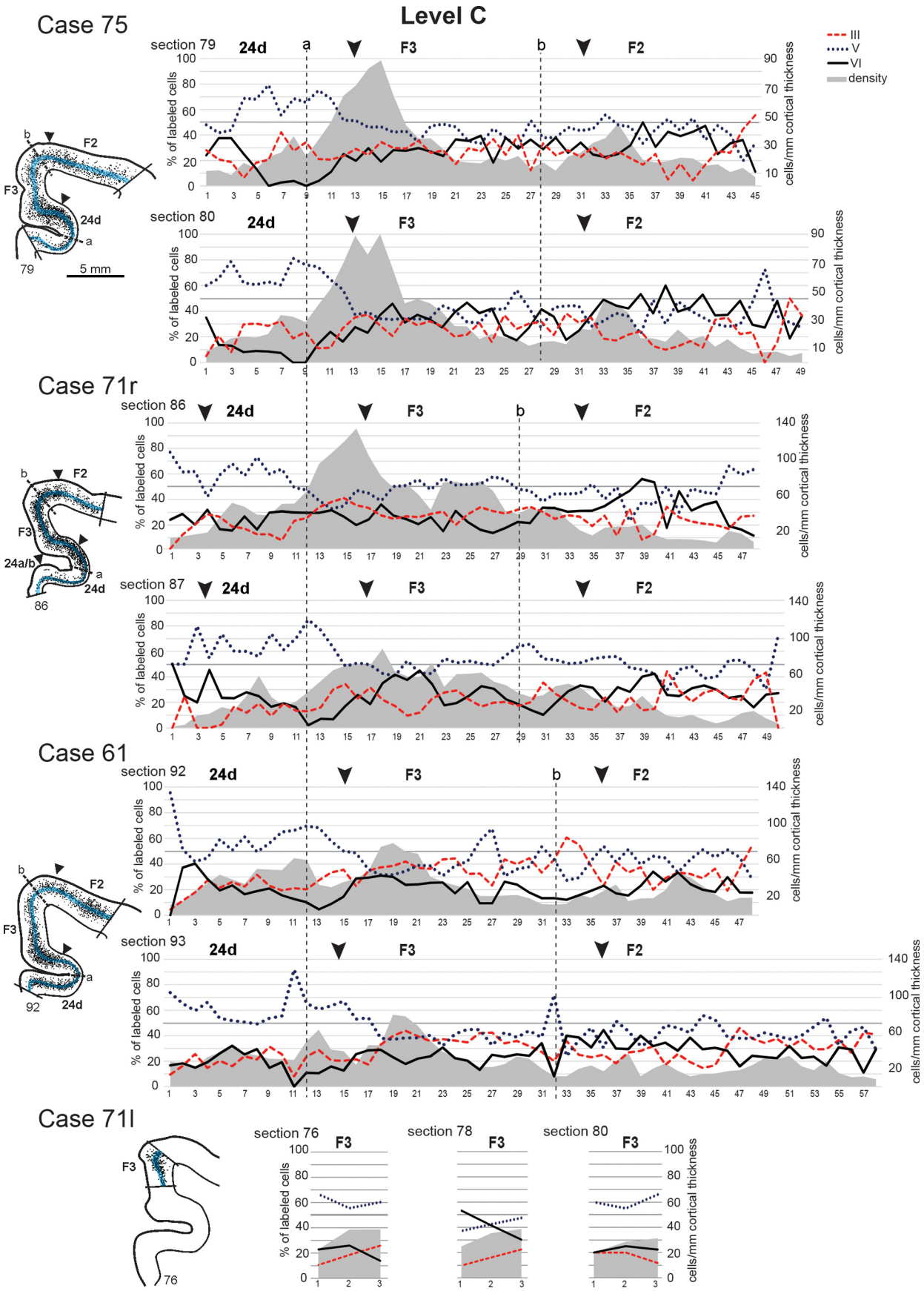

Figure 7. Percent laminar distribution and density of the retrograde labeling in the cingulate and frontal motor cortex at level C in all cases. Conventions as in Figure 4.

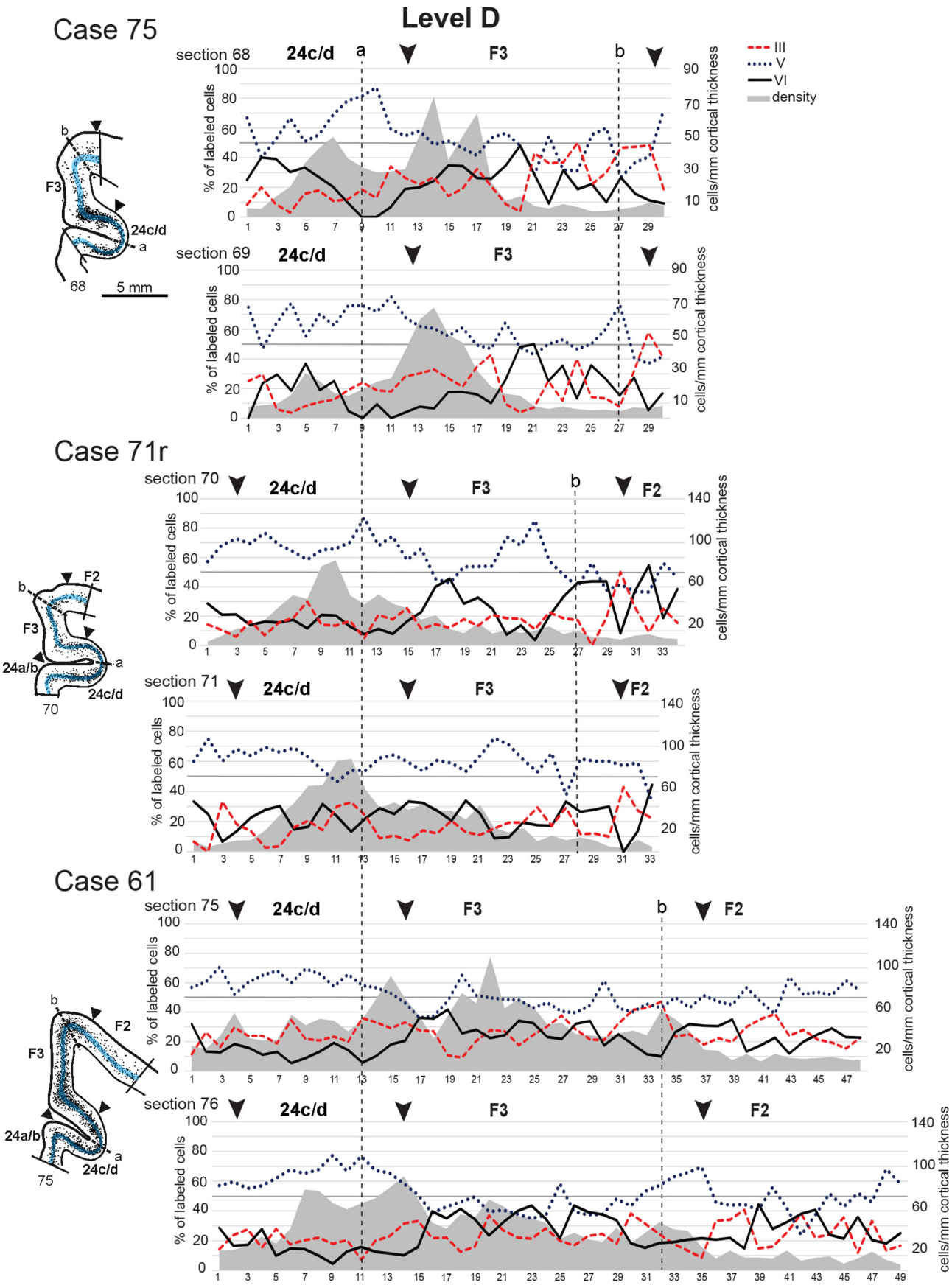

Figure 8. Percent laminar distribution and density of the retrograde labeling in the cingulate and frontal motor cortex at level D in Cases 75, 71r, and 61. Conventions as in Figure 4.

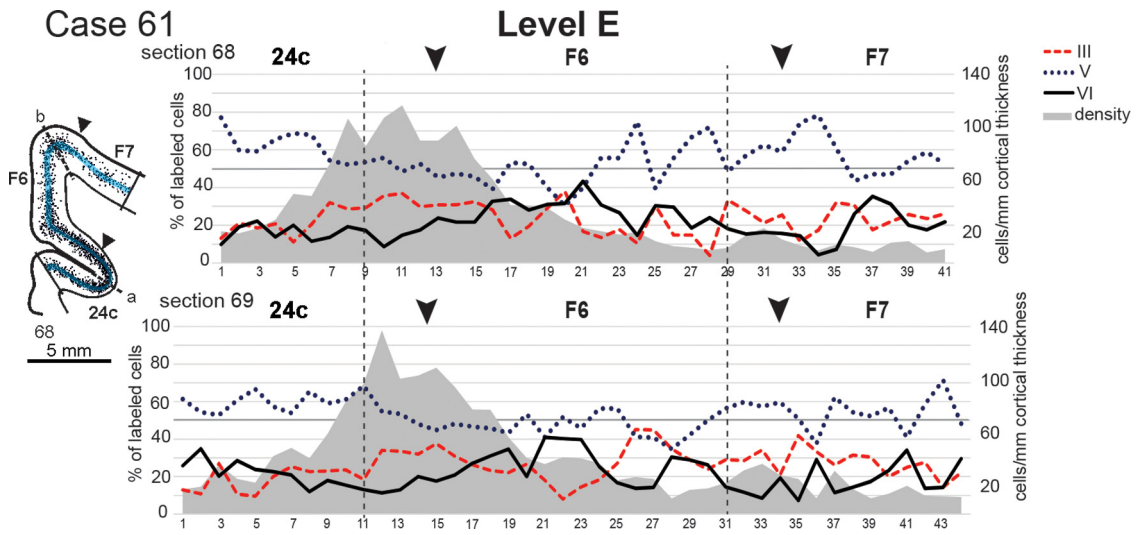

Figure 9. Percent laminar distribution and density of the retrograde labeling in the cingulate and frontal motor cortex at level E in Case 61. Conventions as in Figure 4.

from layer V, as commonly assumed in primate models of CSt interactions, as almost everywhere in these regions the contribution of layers III and VI to these projections is comparable or even stronger than that of layer V. Furthermore, laminar distribution patterns of the CSt projections can largely vary within these regions independently from the richness of the projections and from the projecting area/field, but likely according to the target striatal zones.

Thus, cortical areas appear to project in different ways to different zones of the striatum, so that different striatal zones are targets of characteristically weighted laminar projections from the various input areas. These observations extend current models of CSt interactions and provide an even more complex picture of the possible mode of information processing in the basal ganglia for motor and nonmotor functions.

Laminar origin of CSt projections

The laminar origin of CSt projections has been described in several studies, showing differences across species. In cats, CSt neurons were observed mostly in layer III (Kitai et al., 1976; Oka, 1980; Royce, 1982); whereas in dogs, mostly in layer V or III in PFC and motor cortex, respectively (Tanaka, 1987). In rats, CSt neurons have been observed mostly in layer V, and at a variable extent across studies in layer III (e.g., Veening et al., 1980; McGeorge and Faull, 1989; Akintunde and Buxton, 1992; Wall et al., 2013). In macaques, after putaminal injections, CSt neurons in the motor cortex were described almost exclusively in layer Va (Jones et al., 1977), or primarily in layer Va, but also in layers III and Vb (McFarland and Haber, 2000; Kaneda et al., 2002). After caudate injections, the labeling in PFC was observed primarily in layer V, with a minor contribution from layer III, correlated with labeling density (Arikuni and Kubota, 1986; Goldman-Rakic and Selemon, 1986; Saint-Cyr et al., 1990; Yeterian and Pandya, 1994; Ferry et al., 2000). It is worth noting that, in all these studies, the laminar distribution of CSt-labeled cells has been evaluated only qualitatively, which could be at the basis of an underestimation of the involvement of layers III and VI. Furthermore, the lack of quantitative analysis in virtually all studies of CSt projections prevents comparisons of the contribution of the various layers across different areas, tracer injections, and studies.

The commonly assumed notion that CSt neurons in the macaque brain are primarily located in layer V (Gerfen and Bolam, 2010; Shepherd, 2013) has been challenged by Griggs et al. (2017). This study showed that projections from specific temporal areas to the caudate head originated mostly from layer V and occasionally from layer III, whereas projections from the same areas to the caudate tail originated from layers III and VI. Accordingly, this study first showed that laminar distribution patterns of CSt projections from a given cortical area can markedly differ according to the target striatal zone and that, in macaques, layer VI can be a relevant source of CSt projections.

Present data, based on quantitative analysis of the laminar distribution of CSt neurons, confirm and extend these observations showing that, also in the frontal motor and in the frontal opercular cortex, CSt neurons are not located primarily in layer V and that layer VI can be a major source of CSt projections (e.g., area F5c in Case 61). Labeled CSt neurons in layer VI in ventral premotor cortex were noticed also by McFarland and Haber (2000). Finally, the present data show that, also after tracer injections in different parts of the putamen, different laminar distribution patterns can be observed in a given cortical area. For example, after the injections in Case 61 and in Case 71l, the laminar distribution patterns of the labeled neurons in area F5 were markedly different. Laminar distribution patterns can differ also across different fields of the same area, as observed in F1 and F3. Noteworthy, these patterns did not change depending on the richness of the labeling. Thus, similarly to the temporal cortex, in the motor cortex, laminar distribution patterns of CSt projections appear to vary according to the target striatal zone.

Present data, as well as those of Griggs et al. (2017), raise the question of whether this new model of laminar architecture of CSt projections applies also to other cortical regions. In parietal and cingulate cortex, CSt-labeled cells involved almost exclusively or predominantly layer V. Although the putamen is a major target of CSt parietal projections (Cavada and Goldman-Rakic, 1991; Yeterian and Pandya, 1993), we cannot rule out the possibility that projections to the caudate originate also from other layers. In the insular cortex, we observed labeled CSt neurons in layers V, or V-VI; and Chikama et al. (1997), after injections in the ventral striatum, observed labeling in the agranular insula involving layer III. In the PFC, Griggs et al. (2017) observed differences in CSt projections from layer III to the caudate tail and head; and in the present study, we observed CSt neurons mainly in layers V and VI. Accordingly, it seems possible that, also in the prefrontal and

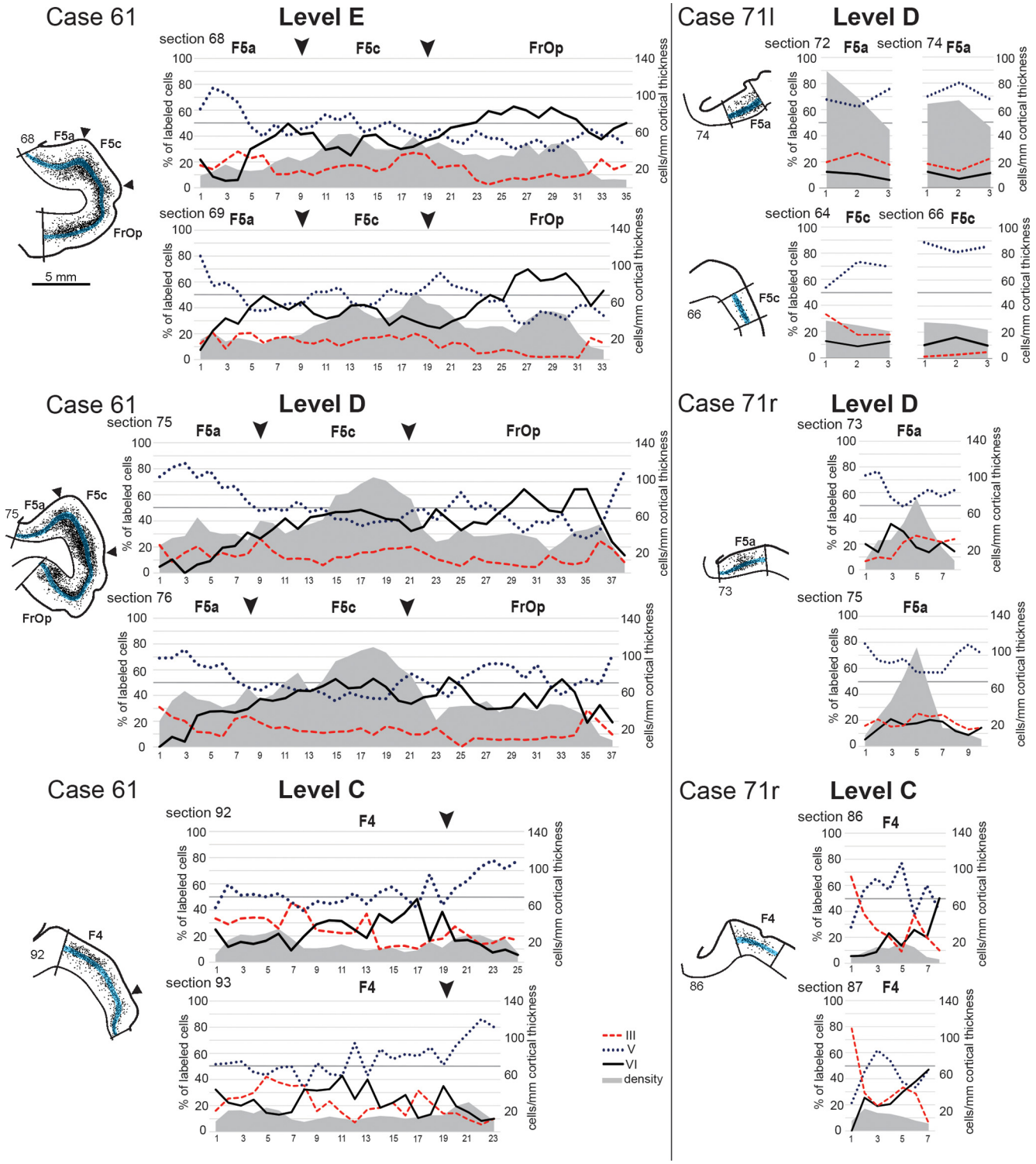

Figure 10. Percent laminar distribution and density of the retrograde labeling in the ventral premotor and opercular frontal cortex. Graphs from Case 61 show data from a cortical region of sections at levels E and D running from the fundus of the arcuate sulcus (left) through F5a, F5c, and the frontal operculum and at level C through F4 on the convexity cortex. Graphs from Case 71l show data from cortical sectors 3-mm-wide of sections taken at level D within the arcuate bank (F5a) or on the convexity cortex (F5c). Graphs from Case 71r show data from cortical sectors taken at level D (in F5a) and level C (in F4) in which the density of labeled cells was >10 cells/bin/mm. Conventions as in Figure 4.

insular cortex, laminar distribution patterns of CSt projections vary according to the target striatal zone.

Functional considerations

Previous data suggested that specific striatal zones are targets of converging input from interconnected cortical areas, thus are integral part of specific large-scale functionally specialized networks (Gerbella et al., 2016; Choi et al., 2017a,b). Present data show that cortical areas may project in different ways to different striatal zones, suggesting that they are targets of specific combinations of signals originating from the various cortical layers of the areas of a given network.

These observations extend current models of CSt interactions, suggesting much more complex modes of information processing in the basal ganglia for different motor and nonmotor functions, and opening new questions on the architecture of the CSt circuitry.

Rodent studies provided evidence for different populations of neurons located in different cortical layers and differentially involved in the CSt circuitry: intrathelencephalic neurons, located in layers III and Va, which also project to other cortical areas, and pyramidal-tract neurons located in layer Vb, which also project to brainstem and spinal cord (Reiner et al., 2010). However, the presence of pyramidal-tract neurons in macaques, suggested by Parent and Parent (2006), is not supported by electrophysiological data (Bauswein et al., 1989). Furthermore, Jones et al. (1977) showed that CSt neurons are smaller than corticospinal neurons and in the present study we have not observed large layer Vb labeled pyramids.

Rodent studies have also provided evidence for inhibitory somatostatin or parvalbumin-positive GABAergic CSt neurons located in layers III, V, and VI (Jinno and Kosaka, 2004; Lee et al., 2014; Rock et al., 2016), which may differentially modulate striatal output and motor activity (Melzer et al., 2017). Although long-range projecting GABAergic cortical neurons have been described in macaques by Tomioka and Rockland (2007), no evidence has been provided so far for inhibitory CSt neurons. Double-labeling experiments will be necessary to verify whether also in the macaque there are inhibitory CSt neurons as observed in rodents.

Current models of cortical circuitry suggest that the various cortical layers display distinct responses and dynamics (see Douglas and Martin, 2004). Specifically, in the premotor cortex, activity generated by thalamic or cortical input first involves the middle layers and then superficial and deep layers (Godlove et al., 2014); and in superficial layers, neural activity is predominantly related to choices, whereas in deeper layers to the motor output (Chandrasekaran et al., 2017). Finally, in frontal areas, deep layers appear to modulate the activity of the superficial layers related to maintaining contents in working memory (Bastos et al., 2018).

Thus, different putaminal zones would collect signals originating from similar sets of hand-related cortical areas, for example, the "lateral grasping network," but differing in term of coding and timing, even when originating from the same area. Furthermore, layers III, V, and VI broadcast signals in different directions (e.g., feed-forward, or feed-back) to other cortical areas of the network. Accordingly, each striatal zone would be involved in a very specific way in the flow of information within the cortico-subcortical network.

In this context, noteworthy is the observation that layer VI can be a robust source of CSt projections. Layer VI hosts pyramidal neurons projecting to the thalamus (corticothalamic, CT) or to other cortical areas (corticocortical, CC; see Thomson, 2010). It is thus an open question whether pyramidal layer VI CSt neurons observed in the present study represent a new class of layer VI pyramids or they belong to the CT and/or the CC types. After tracer injections in the thalamus and in the caudate, Yeterian and Pandya (1994) did not find double-labeled neurons in the PFC, where CSt-labeled cells were observed almost exclusively in layer V. Thus, this study does not rule out the possibility that there are indeed layer VI CSt neurons, which also project to the thalamus. Accordingly, it is possible that striatal zones receive from layer VI neurons signals, which are sent also as feed-back signals either to cortical areas of the network and/or to thalamic nuclei, possibly to the basal ganglia recipient ones. Further studies are necessary to characterize connectionally and neurochemically layer VI CSt neurons and to define the possible role of this projection in the basal ganglia circuitry.

References

Akintunde A, Buxton DF (1992) Origins and collateralization of corticospinal, corticopontine, corticorubral and corticostriatal tracts: a multiple retrograde fluorescent tracing study. Brain Res 586:208–218.

Alexander GE, DeLong MR (1985) Microstimulation of the primate neostriatum: II. Somatotopic organization of striatal microexcitable zones and their relation to neuronal response properties. J Neurophysiol 53:1417–1430.

Alexander GE, DeLong MR, Strick PL (1986) Parallel organization of functionally segregated circuits linking basal ganglia and cortex. Annu Rev Neurosci 9:357–381.

Arikuni T, Kubota K (1986) The organization of prefrontocaudate projections and their laminar origin in the macaque monkey: a retrograde study using HRP-gel. J Comp Neurol 244:492–510.

Bastos AM, Loonis R, Kornblith S, Lundqvist M, Miller EK (2018) Laminar recordings in frontal cortex suggest distinct layers for maintenance and control of working memory. Proc Natl Acad Sci USA 115:1117–1122.

Bauswein E, Fromm C, Preuss A (1989) Corticostriatal cells in comparison with pyramidal tract neurons: contrasting properties in the behaving monkey. Brain Res 493:198–203.

Belmalih A, Borra E, Contini M, Gerbella M, Rozzi S, Luppino G (2009) Multimodal architectonic subdivision of the rostral part (area F5) of the macaque ventral premotor cortex. J Comp Neurol 512:183–217.

Borra E, Gerbella M, Rozzi S, Luppino G (2017) The macaque lateral grasping network: a neural substrate for generating purposeful hand actions. Neurosci Biobehav Rev 75:65–90.

Borra E, Luppino G, Gerbella M, Rozzi S, Rockland KS (2020) Projections to the putamen from neurons located in the white matter and the claustrum in the macaque. J Comp Neurol 528:453–467.

Cavada C, Goldman-Rakic PS (1991) Topographic segregation of corticostriatal projections from posterior parietal subdivisions in the macaque monkey. Neuroscience 42:683–696.

Chandrasekaran C, Peixoto D, Newsome WT, Shenoy KV (2017) Laminar differences in decision-related neural activity in dorsal premotor cortex. Nat Commun 8:614.

Chikama M, McFarland NR, Amaral DG, Haber SN (1997) Insular cortical projections to functional regions of the striatum correlate with cortical cytoarchitectonic organization in the primate. J Neurosci 17:9686–9705.

Choi EY, Ding SL, Haber SN (2017a) Combinatorial inputs to the ventral striatum from the temporal cortex, frontal cortex, and amygdala: implications for segmenting the striatum. eNeuro 4:ENEURO.0392-17.2017.

Choi EY, Tanimura Y, Vage PR, Yates EH, Haber SN (2017b) Convergence of prefrontal and parietal anatomical projections in a connectional hub in the striatum. Neuroimage 146:821–832.

Demelio S, Bettio F, Gobbetti E, Luppino G (2001) Three-dimensional reconstruction and visualization of the cerebral cortex in primates. In: Data visualization (Ebert D, Favre J, Peikert R, eds), pp 147–156. New York: Springer.

Douglas RJ, Martin KA (2004) Neuronal circuits of the neocortex. Annu Rev Neurosci 27:419–451.

Ferry AT, Ongür D, An X, Price JL (2000) Prefrontal cortical projections to the striatum in macaque monkeys: evidence for an organization related to prefrontal networks. J Comp Neurol 425:447–470.

Gerbella M, Borra E, Mangiaracina C, Rozzi S, Luppino G (2016) Corticostriate projections from areas of the "lateral grasping network": evidence for multiple hand-related input channels. Cereb Cortex 26:3096–3078.

Gerfen CR, Bolam P (2010) The neuroanatomical organization of the basal ganglia. In: Handbook of basal ganglia structure and function (Steiner H, Tseng KY, eds), pp 3–32. Amsterdam: Elsevier.

Geyer S, Matelli M, Luppino G, Zilles K (2000) Functional neuroanatomy of the primate isocortical motor system. Anat Embryol (Berl) 202:443–474.

Godlove DC, Maier A, Woodman GF, Schall JD (2014) Microcircuitry of agranular frontal cortex: testing the generality of the canonical cortical microcircuit. J Neurosci 34:5355–5369.

Goldman-Rakic PS, Selemon LD (1986) Topography of corticostriatal projections in nonhuman primates and implications for functional parcellation of the neostriatum. In: Sensory-motor areas and aspects of cortical connectivity (Jones EG, ed), pp 447–466. New York: Plenum.

Griggs WS, Kim HF, Ghazizadeh A, Costello MG, Wall KM, Hikosaka O (2017) Flexible and stable value coding areas in caudate head and tail receive anatomically distinct cortical and subcortical inputs. Front Neuroanat 11:106.

Hof PR, Morrison JH (1995) Neurofilament protein defines regional patterns of cortical organization in the macaque monkey visual system: a quantitative immunohistochemical analysis. J Comp Neurol 352:161–186.

Jinno S, Kosaka T (2004) Parvalbumin is expressed in glutamatergic and GABAergic corticostriatal pathway in mice. J Comp Neurol 477:188–201.

Jones EG, Coulter JD, Burton H, Porter R (1977) Cells of origin and terminal distribution of corticostriatal fibers arising in the sensory-motor cortex of monkeys. J Comp Neurol 173:53–80.

Kaneda K, Nambu A, Tokuno H, Takada M (2002) Differential processing patterns of motor information via striatopallidal and striatonigral projections. J Neurophysiol 88:1420–1432.

Kitai ST, Kocsis JD, Wood J (1976) Origin and characteristics of the corticocaudate afferents: an anatomical and electrophysiological study. Brain Res 118:137–141.

Lanciego JL (2015) Retrograde tract-tracing "plus": adding extra value to retrogradely traced neurons. In: Neural tracing methods: tracing neurons and their connections (Arenkiel BL, ed), pp 67–84. New York: Humana.

Lee AT, Vogt D, Rubenstein JL, Sohal VS (2014) A class of GABAergic neurons in the prefrontal cortex sends long-range projections to the nucleus accumbens and elicits acute avoidance behavior. J Neurosci 34:11519–11525.

Luppino G, Matelli M, Camarda RM, Gallese V, Rizzolatti G (1991) Multiple representations of body movements in mesial area 6 and the adjacent cingulate cortex: an intracortical microstimulation study in the macaque monkey. J Comp Neurol 311:463–482.

Luppino G, Rozzi S, Calzavara R, Matelli M (2003) Prefrontal and agranular cingulate projections to the dorsal premotor areas F2 and F7 in the macaque monkey. Eur J Neurosci 17:559–578.

Matelli M, Luppino G, Rizzolatti G (1985) Patterns of cytochrome oxidase activity in the frontal agranular cortex of macaque monkey. Behav Brain Res 18:125–136.

Matelli M, Luppino G, Rizzolatti G (1991) Architecture of superior and mesial area 6 and the adjacent cingulate cortex in the macaque monkey. J Comp Neurol 311:445–462.

McFarland NR, Haber SN (2000) Convergent inputs from thalamic motor nuclei and frontal cortical areas to the dorsal striatum in the primate. J Neurosci 20:3798–3813.

McGeorge AJ, Faull RL (1989) The organization of the projection from the cerebral cortex to the striatum in the rat. Neuroscience 29:503–537.

Melzer S, Gil M, Koser DE, Michael M, Huang KW, Monyer H (2017) Distinct corticostriatal GABAergic neurons modulate striatal output neurons and motor activity. Cell Rep 19:1045–1055.

Middleton FA, Strick PL (2000) Basal ganglia and cerebellar loops: motor and cognitive circuits. Brain Res Brain Res Rev 31:236–250.

Nambu A (2011) Somatotopic organization of the primate basal ganglia. Front Neuroanat 5:26.

Oka H (1980) Organization of the cortico-caudate projections: a horseradish peroxidase study in the cat. Exp Brain Res 40:203–208.

Parent M, Parent A (2006) Single-axon tracing study of corticostriatal projections arising from primary motor cortex in primates. J Comp Neurol 496:202–213.

Reiner A, Hart NM, Lei W, Deng Y (2010) Corticostriatal projection neurons: dichotomous types and dichotomous functions. Front Neuroanat 4:142.

Reveley C, Gruslys A, Ye FQ, Samaha J, Glen D, Russ B, Saad Z, Seth A, Leopold DA, Saleem KS (2017) Three-dimensional digital template atlas of the macaque brain. Cereb Cortex 27:4463–4477.

Rock C, Zurita H, Wilson C, Apicella AJ (2016) An inhibitory corticostriatal pathway. Elife 5:9.

Royce GJ (1982) Laminar origin of cortical neurons which project upon the caudate nucleus: a horseradish peroxidase investigation in the cat. J Comp Neurol 205:8–29.

Rozzi S, Calzavara R, Belmalih A, Borra E, Gregoriou GG, Matelli M, Luppino G (2006) Cortical connections of the inferior parietal cortical convexity of the macaque monkey. Cereb Cortex 16:1389–1417.

Saint-Cyr JA, Ungerleider LG, Desimone R (1990) Organization of visual cortical inputs to the striatum and subsequent outputs to the pallido-nigral complex in the monkey. J Comp Neurol 298:129–156.

Shepherd GM (2013) Corticostriatal connectivity and its role in disease. Nat Rev Neurosci 14:278–291.

Strick PL, Dum RP, Picard N (1995) Macro-organization of the circuits connecting the basal ganglia with the cortical motor areas. In: Models of information processing in the basal ganglia (Houk G, ed), pp 117–130. Cambridge, MA: MIT Press.

Takada M, Tokuno H, Nambu A, Inase M (1998) Corticostriatal projections from the somatic motor areas of the frontal cortex in the macaque monkey: segregation versus overlap of input zones from the primary motor cortex, the supplementary motor area, and the premotor cortex. Exp Brain Res 120:114–128.

Tanaka D Jr (1987) Differential laminar distribution of corticostriatal neurons in the prefrontal and pericruciate gyri of the dog. J Neurosci 7:4095–4106.

Thomson AM (2010) Neocortical layer 6, a review. Front Neuroanat 4:13.

Tomioka R, Rockland KS (2007) Long-distance corticocortical GABAergic neurons in the adult monkey white and gray matter. J Comp Neurol 505:526–538.

Veening JG, Cornelissen FM, Lieven PA (1980) The topical organization of the afferents to the caudatoputamen of the rat: a horseradish peroxidase study. Neuroscience 5:1253–1268.

Wall NR, De La Parra M, Callaway EM, Kreitzer AC (2013) Differential innervation of direct- and indirect-pathway striatal projection neurons. Neuron 79:347–360.

Yeterian EH, Pandya DN (1993) Striatal connections of the parietal association cortices in rhesus monkeys. J Comp Neurol 332:175–997.

Yeterian EH, Pandya DN (1994) Laminar origin of striatal and thalamic projections of the prefrontal cortex in rhesus monkeys. Exp Brain Res 99:383–398.